Acta Crystallographica Section D
Biological Crystallography
ISSN 0907-4449

A case of structure determination using pseudosymmetry

Sergei Radaev,[a] Johnson Agniswamy[b] and Peter D. Sun[a]*

[a]Structural Immunology Section, Laboratory of Immunogenetics, National Institute of Allergy and Infectious Diseases, National Institutes of Health, 12441 Parklawn Drive, Rockville, Maryland 20852, USA, and [b]Department of Biology, Georgia State University, PO Box 4010, Atlanta, GA 30302, USA

Correspondence e-mail: psun@nih.gov

Received 7 July 2009
Accepted 30 September 2009

Here, a case is presented of an unusual structure determination which was facilitated by the use of pseudosymmetry. Group A streptococcus uses cysteine protease Mac-1 (also known as IdeS) to evade the host immune system. Native Mac-1 was crystallized in the orthorhombic space group $P2_12_12$. Surprisingly, crystals of the inactive C94A mutant of Mac-1 displayed monoclinic symmetry with space group $P2_1$, despite the use of native orthorhombic Mac-1 microcrystals for seeding. Attempts to solve the structure of the C94A mutant by MAD phasing in the monoclinic space group did not produce an interpretable map. The native Patterson map of the C94A mutant showed two strong peaks along the (1 0 1) diagonal, indicating possible translational pseudosymmetry in space group $P2_1$. Interestingly, one-third of the monoclinic reflections obeyed pseudo-orthorhombic $P2_12_12$ symmetry similar to that of the wild-type crystals and could be indexed and processed in this space group. The pseudo-orthorhombic and monoclinic unit cells were related by the following vector operations: $\mathbf{a}_m = \mathbf{b}_o - \mathbf{c}_o$, $\mathbf{b}_m = \mathbf{a}_o$ and $\mathbf{c}_m = -2\mathbf{c}_o - \mathbf{b}_o$. The pseudo-orthorhombic subset of data produced good SAD phases, leading to structure determination with one monomer in the asymmetric unit. Subsequently, the structure of the Mac-1 mutant in the monoclinic form was determined by molecular replacement, which showed six molecules forming three translationally related dimers aligned along the (1 0 1) diagonal. Knowing the geometric relationship between the pseudo-orthorhombic and the monoclinic unit cells, all six molecules can be generated in the monoclinic unit cell directly without the use of molecular replacement. The current case provides a successful example of the use of pseudosymmetry as a powerful phase-averaging method for structure determination by anomalous diffraction techniques. In particular, a structure can be solved in a higher pseudosymmetry subcell in which an NCS operator becomes a crystallographic operator. The geometrical relationships between the subcell and parental cell can be used to generate a complete molecular representation of the parental asymmetric unit for refinement.

1. Introduction

Protein molecules packed in a crystal lattice are often related by non-crystallographic symmetries (NCS) that can benefit their structure determination. Most NCS are rotational in nature and can be applied easily through a density-modification process to improve the quality of experimental electron-density maps. Translational NCS can be detected in native Patterson maps, but their application during density modification is usually not very efficient. When NCS operators are close to true crystallographic symmetry this gives rise to pseudosymmetry (Zwart, Grosse-Kunstleve *et al.*, 2008). Pseudosymmetry can cause some difficulties in determining crystal structures (Dauter *et al.*, 2005; Zwart, Grosse-Kunstleve *et al.*, 2008). On the other hand, the proper incorporation of pseudosymmetry can benefit structure determination in molecular replacement (Navaza *et al.*, 1998). Here, we describe a case in which the use of pseudosymmetry was critical in the structure determination of a group A streptococcus (GAS) protein named Mac-1.

Group A streptococcus (GAS) causes a number of infections ranging from strep throat to streptococcal toxic shock syndrome (Cunningham, 2000). Several virulence factors contribute to the pathogenesis of GAS, among which are recently discovered secreted proteins named Mac-1 and Mac-2 (also known as IdeS) that show limited homology to the α subunit of the human leukocyte adhesion glycoprotein Mac-1 (von Pawel-Rammingen *et al.*, 2002; Lei *et al.*, 2000, 2001). Recently, it has been shown that Mac-1 possesses IgG endopeptidase activity that helps GAS to evade the host immune system (Agniswamy *et al.*, 2004; Lei *et al.*, 2002; von Pawel-Rammingen *et al.*, 2002). It recognizes the lower hinge region of human IgG between the C_H1 and C_H2 domains. To understand the molecular mechanism of Mac-mediated pathogenesis, we determined the crystal structure of SeMet-derivatized Mac-1 using a nonconventional method. Specifically, attempts to phase the structure of the C94A mutant of Mac-1 in its true monoclinic space group did not produce traceable electron-density maps after twofold rotational NCS averaging. However, the presence of both rotational and translational local symmetry formed a pseudo-orthorhombic symmetry and allowed us to phase one-third of the monoclinic reflections in the pseudo-orthorhombic space group. This resulted in an interpretable electron-density map that was good enough for nearly complete chain tracing. This partially refined model was then used to phase the entire monoclinic data set by molecular replacement, which located six molecules in the asymmetric unit. In addition, the geometric relationship between the real monoclinic cell and the pseudo-orthorhombic cell allowed the generation of a complete model by applying corresponding symmetry operations. We suggest that in some cases the presence of pseudo-symmetry can facilitate crystal phasing and structure determination.

Table 1
Data-collection and refinement statistics.

Values in parentheses are for the highest resolution bin.

	Wild-type Mac-1 (PDB code 2au1)	Pseudo-orthorhombic C94A mutant of Mac-1	Monoclinic C94A mutant of Mac-1 (PDB code 2avw)
Data collection			
Space group	$P2_12_12$	$P2_12_12$	$P2_1$
Unit-cell parameters	a = 63.9, b = 87.1, c = 57.6	a = 65.5, b = 94.5, c = 49.8	a = 107.0, b = 65.5, c = 137.2, β = 105.8
Resolution limits (Å)	20–2.4 (2.5–2.4)	20–2.0 (2.1–2.0)	20–2.0 (2.1–2.0)
Total observations	74919	116864	287746
Unique reflections	11918	19911	114364
Completeness (%)	90.4 (50.3)	94.1 (67.9)	92.8 (75.3)
$R_{\rm merge}$† (%)	11.3 (31.4)	7.7 (36.7)	8.1 (33.9)
$\langle I/\sigma(I)\rangle$	14.4 (2.0)	19.0 (2.4)	13.5 (1.5)
Refinement			
Resolution (Å)	20–2.4		20–2.0
No. of protein atoms	2321		13901
No. of solvent atoms	96		995
$R_{\rm cryst}$ (%)	21.6		21.8
$R_{\rm free}$ (%)	26.6		26.7
Mean B factor (Å^2)	33.4		35.1
R.m.s.d. bond lengths (Å)	0.009		0.009
R.m.s.d. bond angles (°)	1.3		1.4

† $R_{\rm merge} = 100 \times \sum_{hkl}\sum_i |I_i(hkl) - \langle I(hkl)\rangle| / \sum_{hkl}\sum_i I_i(hkl)$, where $\langle I(hkl)\rangle$ is the mean intensity of multiple measurements of symmetry-equivalent reflections.

2. Materials and methods

2.1. Protein crystallization and data collection

Recombinant Mac-1 protein, its C94A mutant and the SeMet version of the C94A mutant were overexpressed and purified as described previously (Lei *et al.*, 2002). Wild-type Mac-1 single crystals were obtained by vapor diffusion in hanging drops with reservoir solution containing 1.3 *M* ammonium sulfate and 0.1 *M* sodium citrate pH 4.8. The C94A mutant of Mac-1 and its SeMet analog were grown by microseeding with the wild-type orthorhombic crystals in hanging drops at room temperature with 1.5 *M* ammonium sulfate and 0.1 *M* sodium citrate pH 4.8 as precipitant. The cryoprotectant used for the wild-type and C94A mutant crystals contained 0.8 *M* lithium sulfate, 0.1 *M* sodium citrate pH 4.8 and 25% glycerol. Diffraction data were collected at 100 K on beamline 22-ID of the Southeast Regional Collaborative Access Team (SER-CAT) at the Advanced Photon Source, Argonne National Laboratory (a list of supporting institutions can be found at http://www.ser-cat.org/members.html). The SeMet derivative of C94A mutant of Mac-1 was used to collect multiwavelength anomalous diffraction data at three wavelengths. All data were integrated and scaled with *HKL*-2000 (Otwinowski & Minor, 1997).

3. Results and discussion

3.1. Seeding mutant Mac-1 with the wild-type orthorhombic microcrystals produced monoclinic crystals

Wild-type Mac-1 crystallized in the orthorhombic space group $P2_12_12$, with unit-cell parameters a = 63.9, b = 87.1, c = 57.6 Å and one molecule in each asymmetric unit. The crystals diffracted to 2.4 Å resolution (Table 1). As a step towards crystallization of the complex between Mac-1 and human antibody, a catalytically inactive mutant of Mac-1 was generated by mutating the active-site Cys94 to alanine (C94A). Initial attempts to crystallize the C94A mutant of Mac-1 failed. Subsequently, crystals of C94A were obtained by microseeding using the wild-type orthorhombic microcrystals. Although C94A crystals grew from the wild-type Mac-1 seeds, the mutant Mac-1 crystals belonged to the monoclinic space group $P2_1$ rather than the orthorhombic space group and had unit-cell parameters a = 107.0, b = 65.5, c = 137.2 Å, β = 105.8°. They diffracted to 2.0 Å resolution with six molecules per asymmetric unit. The monoclinic symmetry was further confirmed by data processing (Table 1). In addition, the SeMet derivative of the C94A mutant also crystallized in the monoclinic space group. Mutations or heavy-atom derivatizations are known to cause changes in crystal symmetry. For example, SeMet derivatization of orotidine-5′-monophosphate decarboxylase caused a change in the symmetry from $P2_12_12_1$ to $P2_1$ with a quadrupled unit-cell volume (Poulsen *et al.*, 2001). However, it is unusual to obtain crystals with a symmetry differing from that of the seeds in a microseeding experiment.

3.2. Phasing the C94A Mac-1 data in the monoclinic space group

The Mac-1 sequence contains four methionine residues and with six molecules in the asymmetric unit both *SHELXD* (Sheldrick, 2008) and *Shake-n-Bake* (*SnB*; Weeks & Miller, 1999) readily identified 18 of 24 possible Se sites in the SeMet derivative. This resulted in an overall figure of merit (FOM) of 0.20 and a phasing density map that lacked any traceable features (Fig. 1*a*). In addition, twofold non-crystallographic symmetry (NCS) relating the 18 Se sites was also identified by *SOLVE*/*RESOLVE* (Terwilliger & Berendzen, 1999).

However, addition of the twofold NCS averaging in density modification did not significantly improve the quality of the map (Fig. 1*b*).

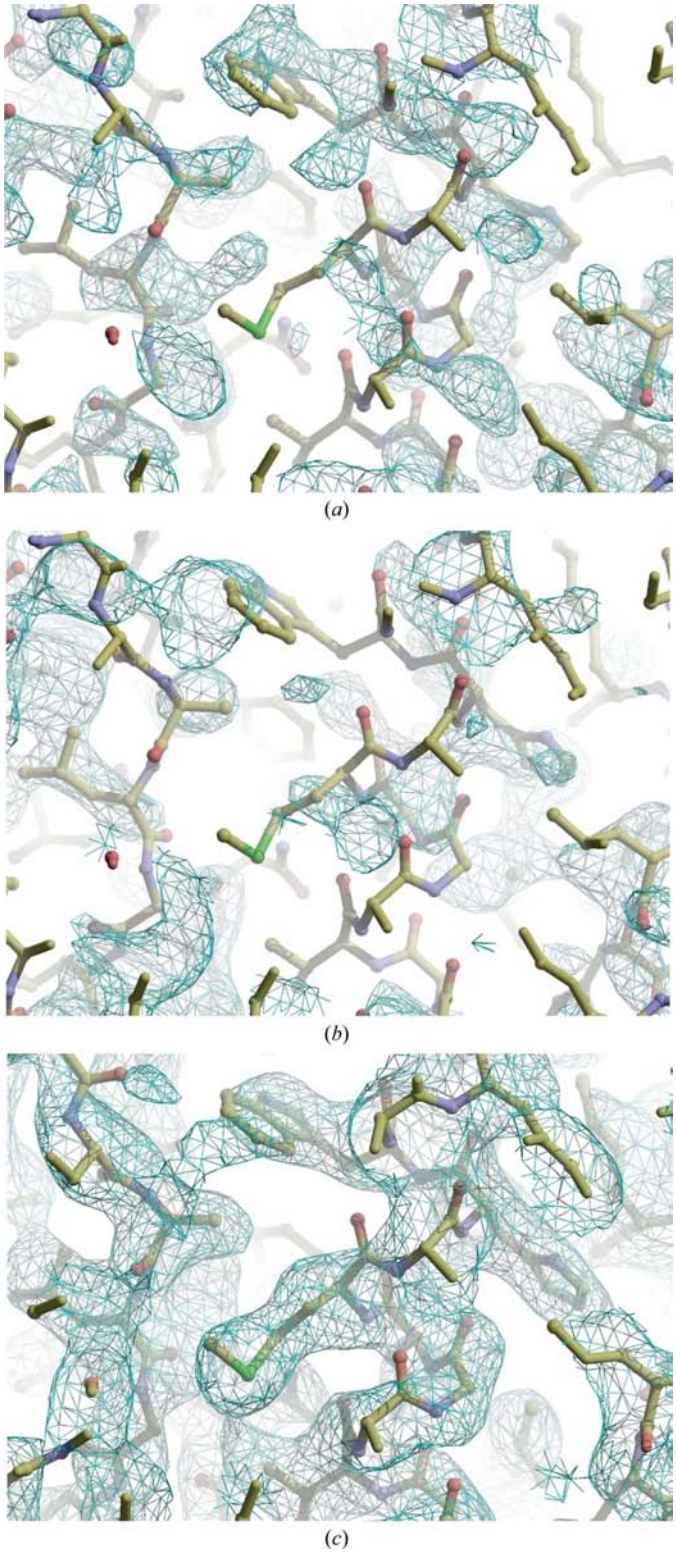

Figure 1
Experimental electron-density maps from Mac-1 crystals. (*a*) Electron-density map of the monoclinic C94A Mac-1 mutant calculated using MAD phases. (*b*) Twofold NCS-averaged electron-density map of the C94A mutant calculated using MAD phases. (*c*) Electron-density map of the C94A mutant calculated using SAD phases in the pseudo-orthorhombic space group.

3.3. Twinning analysis and reindexing of the C94A Mac-1 data using pseudo-orthorhombic symmetry

The facts that C94A mutant Mac-1 crystals could only be obtained from seeding with the wild-type orthorhombic crystals and that the length of the monoclinic **b** axis ($\mathbf{b}_m$) was very similar to the wild-type orthorhombic **a** axis ($\mathbf{a}_o$) prompted us to closely examine the

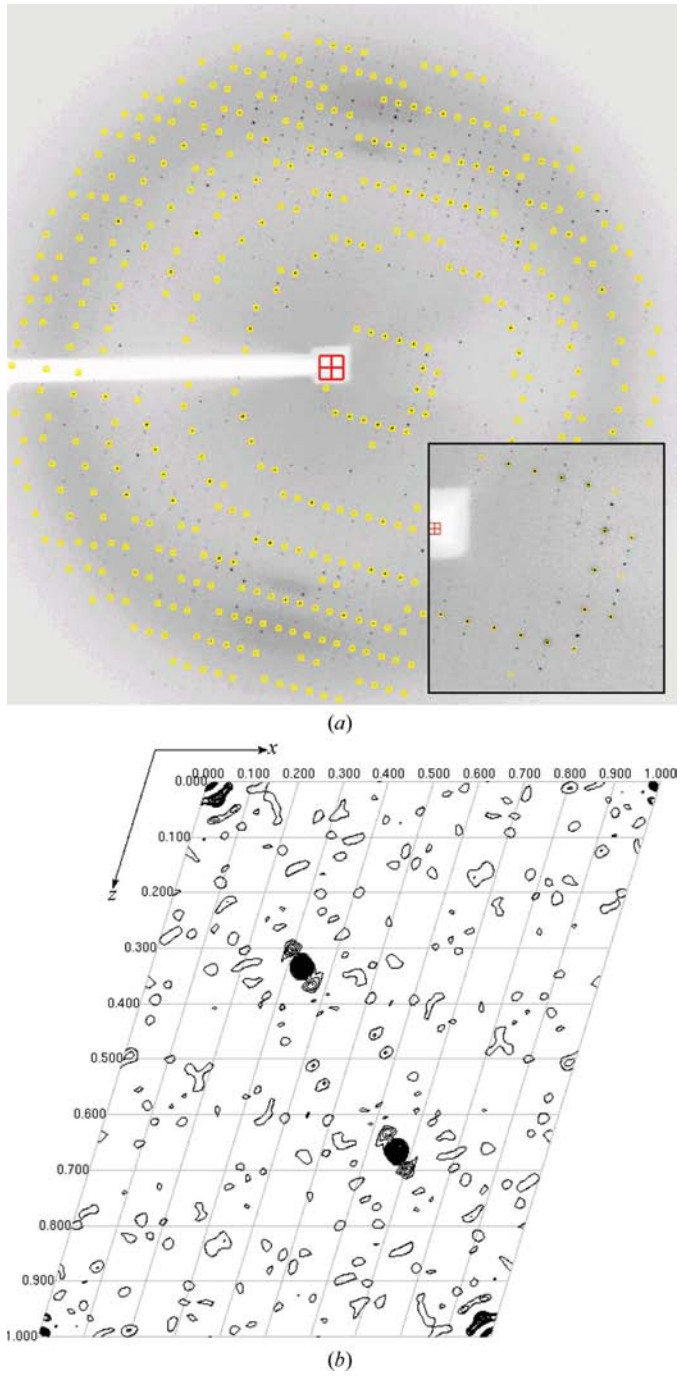

Figure 2
Experimental data indicating the presence of pseudosymmetry in monoclinic crystals of the Mac-1 C94A mutant. (*a*) A diffraction image of a monoclinic crystal of the C94A mutant of Mac-1 indexed in pseudo-orthorhombic symmetry (yellow circles). Only one-third of all reflections were indexed in this case. The insert shows an enlarged portion of the image. (*b*) Native Patterson showing the $y = 0$ plane in the monoclinic space group. There are two additional peaks indicating translational symmetry along the (1 0 1) axis of the cell. This figure was prepared using the *CCP*4 software package (Collaborative Computational Project, Number 4, 1994).

monoclinic diffraction data. While the diffraction of C94A Mac-1 clearly confirmed a monoclinic spacing, the diffraction pattern appeared to consist of three sets of similar reflections spaced along the (1 0 1) direction, with one set, namely every third reflection, being systematically stronger than the two weaker sets, which resembled the strong set in intensity distribution (Fig. 2*a*). In addition, the native Patterson map showed the presence of a strong peak at a position ±1/3 along the (1 0 1) diagonal with a height of 57% of the origin peak (Fig. 2*b*). Taking all this information into account, we decided to re-index the data set. By cutting down the number of reflections in the peak-search procedure of *HKL*-2000 (Otwinowski & Minor, 1997), we ended up with about 30 strongest reflections. Based on these peaks, one-third of the reflections in the monoclinic space group could be indexed in the orthorhombic space group $P2_12_12$ with unit-cell parameters a = 65.5, b = 94.5, c = 49.8 Å (Table 1). The unit-cell parameters and symmetry of this pseudo-orthorhombic space group are similar to those found in the wild-type crystals of Mac-1. In fact, the monoclinic and the orthorhombic unit cells are related through the vector operations $\mathbf{a}_m = \mathbf{b}_o - \mathbf{c}_o$, $\mathbf{b}_m = \mathbf{a}_o$ and $\mathbf{c}_m = -2\mathbf{c}_o - \mathbf{b}_o$, with the volume of the monoclinic cell being three times larger than that of the pseudo-orthorhombic cell (Fig. 3*a*). The presence of a subset of reflections displaying higher symmetry raises the possibility of merohedral twinning. Therefore, a series of twinning tests implemented in the program *phenix.xtriage* (Zwart, Afonine *et al.*, 2008) were carried out on both the whole monoclinic data set and the orthorhombic subset of reflections. Depending on the degree of twinning, the twinning index $\langle I^2\rangle/\langle I\rangle^2$ varies between 1.5 for perfectly twinned data and 2 for untwinned data (Yeates, 1997). The $\langle I^2\rangle/\langle I\rangle^2$ value was 1.926 for acentric reflections in $P2_12_12$ symmetry, indicating a lack of twinning in the crystal. The absence of any detectable merohedral twinning was further supported by analysis of the $\langle F\rangle^2/\langle F^2\rangle$ and $\langle|E^2-1|\rangle$ values from the program *phenix.xtriage* (Table 2). Another way of detecting the presence of 222 symmetry in the monoclinic space group is through analysis of the normalized structure factors E. In particular, theoretical calculations show that centric reflections produce an average value of $|E^2-1|$ close to 1, while noncentrosymmetric reflections would give a smaller value of 0.74 (Stout & Jensen, 1989). Normally, in space group $P2_1$ one should expect to find one centric zone $k_m = 0$. However, strong $P2_12_12$ pseudosymmetry implies that in the monoclinic space group, besides $k_m = 0$, which corresponds to $h_o = 0$ (Fig. 3), there should be two additional centric zones in the monoclinic data set: $2h_m = l_m$ (equivalent to $k_o = 0$) and $h_m = -l_m$ (equivalent to $l_o = 0$). Indeed, the calculations show that the average $|E^2-1|$ is equal to 1.09, 1.01 and 1.43 for $k_m = 0$, $h_m = -l_m$ and $2h_m = l_m$, respectively. This further validates the presence of two additional centric planes and thus the 222 symmetry within the monoclinic space group.

After re-indexing a subset of the monoclinic SeMet data in the pseudo-orthorhombic unit cell, all four predicted Se sites except for the N-terminal one belonging to the single molecule in the asymmetric unit were easily identified by *SHELXD* and *SnB*, resulting in an FOM of 0.32. The SAD map after density modification using the peak-wavelength SeMet data was readily interpretable (Fig. 1*c*). It was possible to build a near-complete model into the density and refine it partially to R_{cryst} = 29.5% and R_{free} = 35.4%. This partially refined Mac-1 structure was used as the model to phase the entire data set in the monoclinic space group by molecular replacement. The refined R factors in $P2_1$ were R_{cryst} = 21.8% and R_{free} = 26.7%.

Table 2
Reflection statistics for C94A MAC-1 crystals in monoclinic and pseudo-orthorhombic settings calculated by *phenix.xtriage*.

	Space group		Theoretical values	
	$P2_1$	$P2_12_12$	Untwinned	Perfect twin
Acentric reflections				
$\langle I^2\rangle/\langle I\rangle^2$	2.397	1.926	2.000	1.500
$\langle F\rangle^2/\langle F^2\rangle$	0.757	0.805	0.785	0.885
$\langle\|E^2-1\|\rangle$	0.800	0.701	0.736	0.541
Centric reflections				
$\langle I^2\rangle/\langle I\rangle^2$	3.645	2.781	3.000	2.000
$\langle F\rangle^2/\langle F^2\rangle$	0.618	0.688	0.637	0.785
$\langle\|E^2-1\|\rangle$	1.024	0.936	0.968	0.736
Mean $\|L\|$	0.476	0.468	0.500	0.375
Mean L^2	0.306	0.298	0.333	0.200

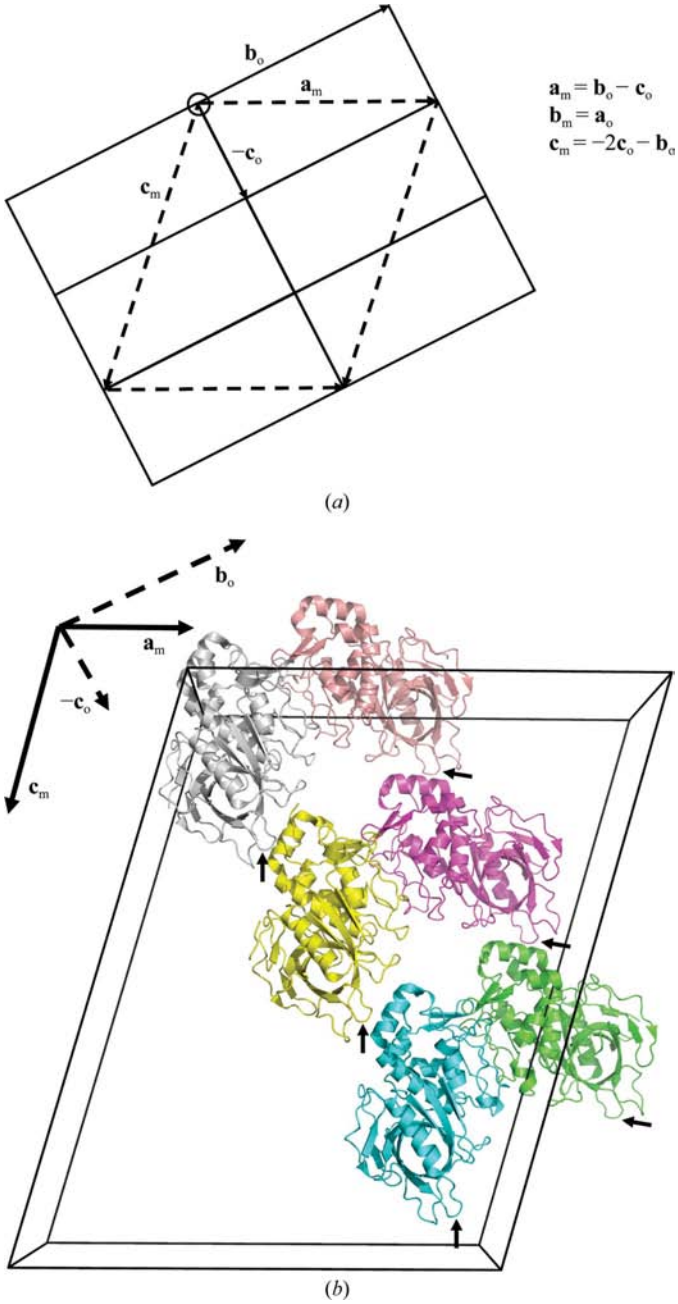

Figure 3
(*a*) A schematic drawing showing the geometrical relations between the monoclinic and pseudo-orthorhombic unit cells. Axis $\mathbf{b}_m$ is pointing out of the plane. (*b*) Mac-1 molecule packing in the monoclinic space group. The loops between residues 300 and 305 that show largest degree of flexibility between monomers are indicated by arrows. This figure was prepared using the program *PyMOL* (DeLano, 2002).

Table 3
Refinement of the pseudoorthorhombic structural model in the subgroups of $P2_12_12$.

Space group	Operators used to generate NCS-related molecules	R_{cryst}	R_{free}
$P2_12_12$	None	29.5	35.4
$P112$	$(\frac{1}{2}+x, \frac{1}{2}-y, -z)$	31.0	36.8
$P12_11$†	$(-x, -y, z)$	32.0	38.4
$P2_111$‡	$(-x, -y, z)$	32.3	38.7
$P1$	$(-x, -y, z)$, $(\frac{1}{2}+x, \frac{1}{2}-y, -z)$, $(\frac{1}{2}-x, \frac{1}{2}+y, -z)$	31.6	38.9

† The coordinates of the original molecule and its NCS-related mate should be shifted by $(\frac{1}{4}, 0, 0)$ to account for the differences in origin conventions between space groups $P2_12_12$ and $P12_11$. ‡ The coordinates of the original molecule and its NCS-related mate should be shifted by $(0, \frac{1}{4}, 0)$ to account for differences in origin conventions between space groups $P2_12_12$ and $P2_111$.

3.4. The molecular packing underlining the pseudosymmetry

The packing of C94A Mac-1 in the monoclinic unit cell shows that there are six molecules in each asymmetric unit, forming three translationally related dimers along the (1 0 1) diagonal of the monoclinic space group (Fig. 3). The two monomers in each dimer are related by a noncrystallographic twofold axis. This twofold NCS becomes a crystallographic twofold along the pseudo-orthorhombic **c** axis, the unit-cell length of which equals the pseudotranslation between the dimers along the (1 0 1) direction of the monoclinic cell (Fig. 3). The unique 2_1 screw axis **b** in the monoclinic cell forms the **a** axis in the pseudo-orthorhombic cell. Thus, both rotational and translational NCS in the monoclinic space group have become crystallographic symmetries in the pseudo-orthorhombic space group. This *de facto* introduces sixfold averaging, three translational and two rotational, into the phases, which improved the electron density considerably. Further structure comparison among the three translationally related dimers showed that minor conformational differences exist in several loop regions (mostly for residues 300–305; Fig. 3*b*) between the dimers (r.m.s.d.s in the range 0.2–0.6 Å in pairwise comparison), rendering them non-identical and thus breaking true crystallographic orthorhombic space-group symmetry.

3.5. Analysis of the pseudosymmetry

The pseudo-orthorhombic space group observed in the monoclinic Mac-1 crystal is a combination of the crystallographic 2_1 symmetry (along the pseudo-orthorhombic **a** axis) with a twofold NCS and a translational symmetry both along the (1 0 1) direction. Since the 2_1 screw axis remains a crystallographic axis, this suggests that either the twofold NCS or the translation or both are imperfect and are thus the source of pseudosymmetry. To delineate the source of the pseudosymmetry, we carried out several refinements in subgroups of the $P2_12_12$ space group, *i.e.* $P112$, $P2_111$ and $P12_11$. If the pseudosymmetry is generated by the twofold axis, refinement in $P112$ and $P2_12_12$ would result in worse R factors than that in $P2_111$, a true crystallographic symmetry that is retained in both the monoclinic and pseudo-orthorhombic cells. For the refinements in the subgroups of the $P2_12_12$ space group additional molecules related by NCS symmetry were generated and in some cases the axes were reoriented, the origin was shifted and the reflections were re-indexed to conform to the IUCr conventions (*International Tables for Crystallography*, 2002). The results show that all refinements in the subgroups of $P2_12_12$ resulted in comparable R factors that were also similar to the refinement in space group $P2_12_12$ (Table 3). This indicates that the twofold symmetry is not a pseudosymmetry. To confirm the translational nature of the pseudosymmetry, we carried out a refinement in the monoclinic space group $P2_1$ (large cell) using only the 33% of experimental data that constitute the subset of strong reflections indexed in orthorhombic $P2_12_12$ symmetry. Refinement in space group $P2_1$ (large cell) does not constrain translational symmetry on NCS-related molecules, whereas refinement in the $P2_111$ subgroup (small cell) that uses essentially the same set of reflections does. The comparison shows a significant difference in R factors between the two refinements. Refinement in the large monoclinic cell based on the 33% of reflections (strongest set) yielded a smaller crystallographic R factor (R_{cryst} = 21.6% and R_{free} = 27.4%) than that in the orthorhombic cell (R_{cryst} = 32.3% and R_{free} = 38.7%; Table 3). This indicates that deviations from the higher orthorhombic symmetry are caused mainly by imperfection in translational, not rotational, relations between molecules in the crystal.

3.6. Generating a complete refinement model for the C94A Mac-1 data set by using geometric relationships between the monoclinic and pseudo-orthorhombic unit cells

Although in the original publication molecular replacement was used to find all six molecules in the monoclinic cell (Agniswamy *et al.*, 2006), its use is not necessary given the known geometrical relationships between the monoclinic cell and the pseudo-orthorhombic subcell. Similar procedures have been described previously, for example in Di Costanzo *et al.* (2003) and Zwart, Grosse-Kunstleve *et al.* (2008). In fact, in some cases where molecular replacement would have difficulties, such as low-resolution data or multiple copies of macromolecules in a unit cell, it might be the only way to generate a complete model. The procedure of generation of the complete model in the monoclinic unit cell can be divided into two steps. In the first step the six independent molecules are generated in the pseudo-orthorhombic unit cell. In the second step, an appropriate transformation is applied to bring the six molecules into the monoclinic system of coordinates. To generate the six independent molecules, translational symmetry was applied to generate monomers related by translational pseudosymmetry in the pseudo-orthorhombic cell, *i.e.* $x, y, z+1$ and $x, y, z+2$ (Fig. 3). The twofold crystallographic axis $-x, -y, z$ (which is equivalent to twofold NCS in the monoclinic cell) then completes the generation of the complete model of six molecules. As a next step, the six molecules should be rotated and shifted accordingly to fit into the proper orientation of the monoclinic cell. There is a difference in the origin conventions between the orthorhombic $P2_12_12$ and monoclinic $P2_1$ cells (*International Tables for Crystallography*, 2002). In space group $P2_12_12$ the origin is on the twofold axis in the plane of two intersecting 2_1 axes and is shifted by $\frac{1}{4}$ in the x and y directions from the point of their intersection. In space group $P2_1$ the origin is on 2_1 and is not fixed along this axis. Therefore, the orthorhombic coordinates of the generated molecules should be shifted by $(0, -0.25, 0)$ to account for the origin differences and then transformed based on the relationships between the unit cells (Fig. 3),

$$\mathbf{T} = \begin{pmatrix} 0 \\ -0.25 \\ 0 \end{pmatrix}, \quad \mathbf{R} = \begin{pmatrix} 0 & -0.885 & 0.465 \\ 1 & 0 & 0 \\ 0 & 0.465 & 0.885 \end{pmatrix}.$$

After the transformation, the final coordinates of the six molecules could be easily refined in space group $P2_1$, resulting in R_{cryst} = 29.4% and R_{free} = 37.7%. This is comparable to the result of molecular replacement, in which the R factors were R_{cryst} = 35.7% and R_{free} = 43.8% after the first round of refinement. Representative sections of $2F_o - F_c$ electron densities for the molecules generated by direct coordinate transformation are comparable to corresponding ones derived from molecular replacement (Fig. 4).

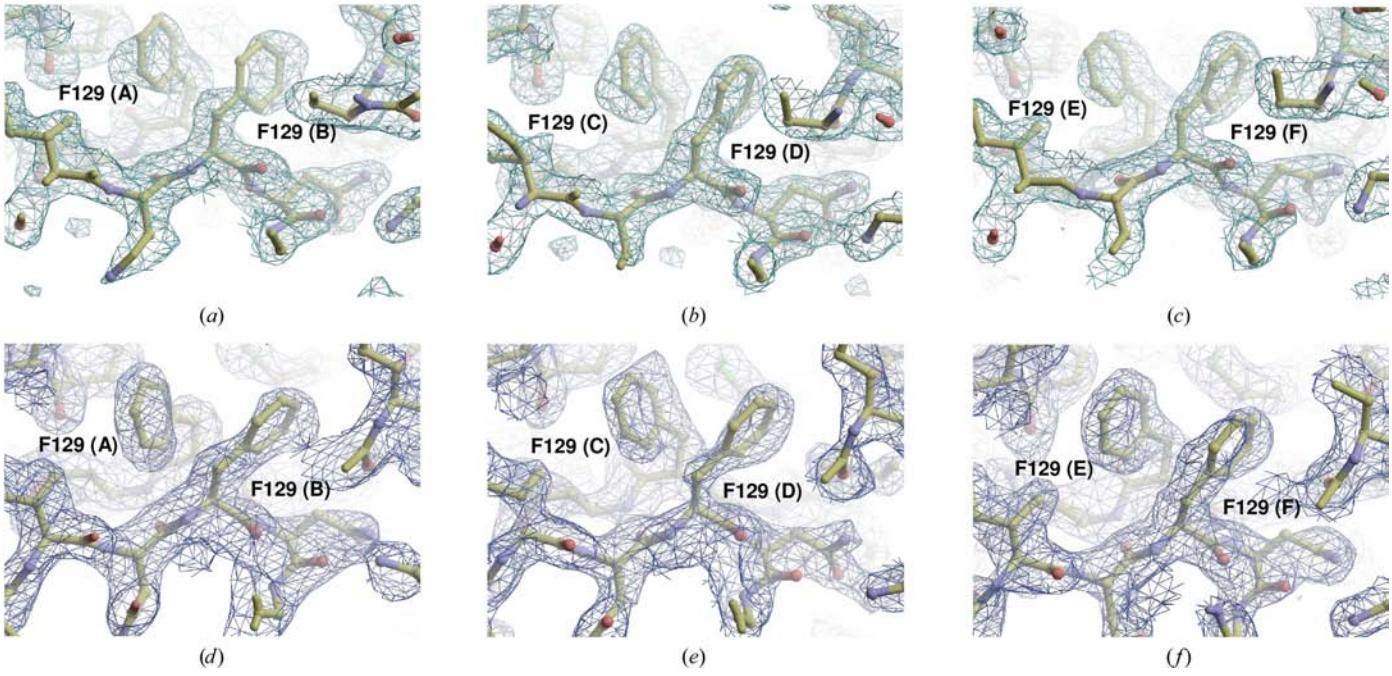

Figure 4
Representative sections of $2F_o - F_c$ electron density for the monoclinic structure models generated by operators as explained in §3.6 (*a*–*c*) or molecular replacement (*d*–*f*). The area around the twofold NCS axis is shown; the chain identifier is indicated in parentheses. Electron density is contoured at the 1.0σ level.

4. Conclusions

The structure of the C94A mutant of Mac-1 in the monoclinic form represents an interesting case in which seeding with orthorhombic wild-type crystals probably caused the monoclinic crystal lattice to maintain pseudo-orthorhombic packing. Interestingly, a subset of strongest reflections containing one-third of all data could be treated as an independent and complete data set that allowed us to obtain better phasing information owing to an equivalent sixfold averaging in the pseudo-orthorhombic cell.

As pointed out by Zwart, Grosse-Kunstleve *et al.* (2008), pseudosymmetry is not an uncommon phenomenon and around 6% of structures deposited in the PDB exhibit it. Pseudosymmetry is simply a special case of NCS in which the NCS operators (both rotational or/and translational) orient themselves relatively close to special directions in the unit cell which would produce almost perfect crystallographic symmetry of higher order. Generally, these special orientations coincide with either principal or diagonal crystallographic axes. Although the resulting diffraction pattern would have the periodicity of a low-symmetry lattice, it will be modulated in a certain way. The presence of pseudosymmetry will produce quasi-systematic absences with weaker reflections following a systematic pattern. Pseudosymmetries can often readily be identified based on Patterson and self-rotation maps. In certain cases, once pseudosymmetry has been identified a subset of the diffraction data can be re-indexed in a higher symmetry space group in which the NCS operator becomes a crystallographic operator to provide better phases for structural solution. The present results show that such an approach can not only be used in molecular replacement, as applied previously by Navaza *et al.* (1998), but also in anomalous diffraction methods. Knowledge of the geometrical relationships between the experimental space group and the pseudo space group of higher symmetry, together with information from the native Patterson and self-rotation function, could be used to generate a complete model. This transformation can be used instead of molecular replacement to position each molecule in the parental experimental space group for refinement.

All X-ray diffraction data were collected on the Southeast Regional Collaborative Access Team (SER-CAT) 22-ID beamline at the Advanced Photon Source, Argonne National Laboratory. Supporting institutions are listed at http://www.ser-cat.org. This research was supported by the intramural research program of National Institute of Allergy and Infectious Diseases, National Institutes of Health.

References

Agniswamy, J., Lei, B., Musser, J. M. & Sun, P. D. (2004). *J. Biol. Chem.* **279**, 52789–52796.
Agniswamy, J., Nagiec, M. J., Liu, M., Schuck, P., Musser, J. M. & Sun, P. D. (2006). *Structure*, **14**, 225–235.
Collaborative Computational Project, Number 4 (1994). *Acta Cryst.* D**50**, 760–763.
Cunningham, M. W. (2000). *Clin. Microbiol. Rev.* **13**, 470–511.
Dauter, Z., Botos, I., LaRonde-LeBlanc, N. & Wlodawer, A. (2005). *Acta Cryst.* D**61**, 967–975.
DeLano, W. L. (2002). *The PyMOL Molecular Graphics System.* http://www.pymol.org.
Di Costanzo, L., Forneris, F., Geremia, S. & Randaccio, L. (2003). *Acta Cryst.* D**59**, 1435–1439.
International Tables for Crystallography (2002). Vol. *A*, *Space Group Symmetry*, 5th ed., edited by T. Hahn. Dordrecht: Kluwer Academic Publishers.
Lei, B., DeLeo, F. R., Hoe, N. P., Graham, M. R., Mackie, S. M., Cole, R. L., Liu, M., Hill, H. R., Low, D. E., Federle, M. J., Scott, J. R. & Musser, J. M. (2001). *Nature Med.* **7**, 1298–1305.
Lei, B., DeLeo, F. R., Reid, S. D., Voyich, J. M., Magoun, L., Liu, M., Braughton, K. R., Ricklefs, S., Hoe, N. P., Cole, R. L., Leong, J. M. & Musser, J. M. (2002). *Infect. Immun.* **70**, 6880–6890.
Lei, B., Mackie, S., Lukomski, S. & Musser, J. M. (2000). *Infect. Immun.* **68**, 6807–6818.
Navaza, J., Panepucci, E. H. & Martin, C. (1998). *Acta Cryst.* D**54**, 817–821.
Otwinowski, Z. & Minor, W. (1997). *Methods Enzymol.* **276**, 307–326.

Pawel-Rammingen, U. von, Johansson, B. P. & Bjorck, L. (2002). *EMBO J.* **21**, 1607–1615.
Poulsen, J.-C. N., Harris, P., Jensen, K. F. & Larsen, S. (2001). *Acta Cryst.* D**57**, 1251–1259.
Sheldrick, G. M. (2008). *Acta Cryst.* A**64**, 112–122.
Stout, G. H. & Jensen, L. H. (1989). *X-Ray Structure Determination: A Practical Guide*, 2nd ed. New York: John Wiley & Sons.
Terwilliger, T. C. & Berendzen, J. (1999). *Acta Cryst.* D**55**, 849–861.
Weeks, C. M. & Miller, R. (1999). *Acta Cryst.* D**55**, 492–500.
Yeates, T. O. (1997). *Methods Enzymol.* **276**, 344–358.
Zwart, P. H., Afonine, P. V., Grosse-Kunstleve, R. W., Hung, L.-W., Ioerger, T. R., McCoy, A. J., McKee, E., Moriarty, N. W., Read, R. J., Sacchettini, J. C., Sauter, N. K., Storoni, L. C., Terwilliger, T. C. & Adams, P. D. (2008). *Methods Mol. Biol.* **426**, 419–435.
Zwart, P. H., Grosse-Kunstleve, R. W., Lebedev, A. A., Murshudov, G. N. & Adams, P. D. (2008). *Acta Cryst.* D**64**, 99–107.